

Petrography and Lithochemistry of the Granitic Rocks from Nattaung Area, Singu Township, Mandalay Region

Myo Min Tun^{1*}, Khin Win Khaing², Zar Ni Swe¹, Thet Naing³

Abstract

The research area is located in the Singu Township, Mandalay Region of Myanmar and belongs to a part of the so-called “Mogok Metamorphic Belt”. It is comprised of metasedimentary and intrusive igneous rocks. This study focuses on the petrological and geochemical analyses of granitic rocks exposed in the Nattaung area in order to explore the petrological and petrochemical characteristics, their origin and genesis. Petrographic examination of the granitic rock samples was carried out under polarizing microscope. Major and trace element composition of the granitic rocks were analyzed by X-Ray Fluorescence. Mineralogical and petrochemical data suggest that the granitic rocks from Nattaung area are classified as S-type granite intruded within the highly deformed metamorphic terrains. Tectonic environments for granitic rocks are discriminated as orogenic granitoids based on major and minor element chemistry.

Key words: Petrography, Lithochemistry, Granite, Nattaung, S-type, Orogenic

Introduction

The research area lies within the Mogok Metamorphic Belt (MMB) (Mitchell, 2007; Searle and Ba Than Haq, 1964). This belt stretches over 1450 km long and up to 40 km wide, as a north-south trending belt consisting of regionally metamorphosed rocks including kyanite and sillimanite schists and granites lying along the Western margin of the Shan Plateau in central Myanmar and continuing as arcuate trend northwards to the eastern Himalayan syntaxis.. It comprises a sequence of high-grade meta-sedimentary and meta-intrusive rocks, representing a regionally metamorphosed amphibolite-grade belt. Metasedimentary rocks and intrusive igneous rocks of MMB are well exposed in the study area. Searle and Ba Than Haq (1964) suggested that the protolith rocks of the MMB spanned from Precambrian to Late Paleozoic. The metamorphism was suggested to be occurred in post-Paleozoic time, almost certainly related to the Himalayan orogeny. Bertrand et al. (1999) reported late Oligocene to early Miocene based on $^{39}\text{Ar}/^{40}\text{Ar}$ ages (ranging from 26.9 ± 1 Ma to 16.6 ± 0.3 Ma) on biotite and muscovite from rocks along the Shan scarp. Barley et al. (2003) reported U-Pb age data from the MMB. They reported the zircon ages of Jurassic, mid-Cretaceous and early Eocene time, confirming that Andean-type granite magmatism was widespread along the Burma margin throughout the pre-collisional period (Mitchell, 1993).

This study focuses on the petrological and geochemical analyses of granitic rocks exposed in the Nattaung area in order to explore the petrological and petrochemical characteristics, their origin and genesis.

Geology of the Nattaung area

Metasedimentary and igneous rocks occur in the study area. The meta-sedimentary rocks include calc-silicate rocks, garnet biotite schist and gneisses, quartzite and various types of marbles such as diopside-forsterite marble, white marble, diopside marble, tremolite-actinolite marble. The igneous rocks comprise of biotite microgranite, syenite, leucogranite,

¹Lecturer, Department of Geology, Yadanabon University

²Geologist, Banmaw, Kachin State

³Professor and Head, Department of Geology, Patheingyi University

and with minor aplite and pegmatite veins. Geological map of the study area is shown in figure 1.

The biotite microgranite, which is the predominant intrusive rock of the study area, is considered to be equivalent unit of Kabaing granite. It is medium-grained granite consisting of quartz, orthoclase, plagioclase, and biotite with accessory muscovite, apatite and iron ores. As the age of Kabaing granite is suggested to be Eocene- Middle Miocene age based on the $^{40}\text{Ar}/^{39}\text{Ar}$ dating of 15.8 ± 1.1 Ma (Eocene-Middle Miocene) (Bertrand et al., 2001). Thus, the granite in the research area is regarded as Eocene-Middle Miocene in age. Northern and eastern parts of the research area are marked by the large exposures of biotite microgranite. In the middle and southern portions of the area, garnet-biotite gneiss, calc-silicate and marble units are largely cropped out. They are often associated with small syenite bodies along the contact with biotite microgranite. Exposures of other rock units such as garnet mica schist, and quartzite occurs in the southern part of the area.

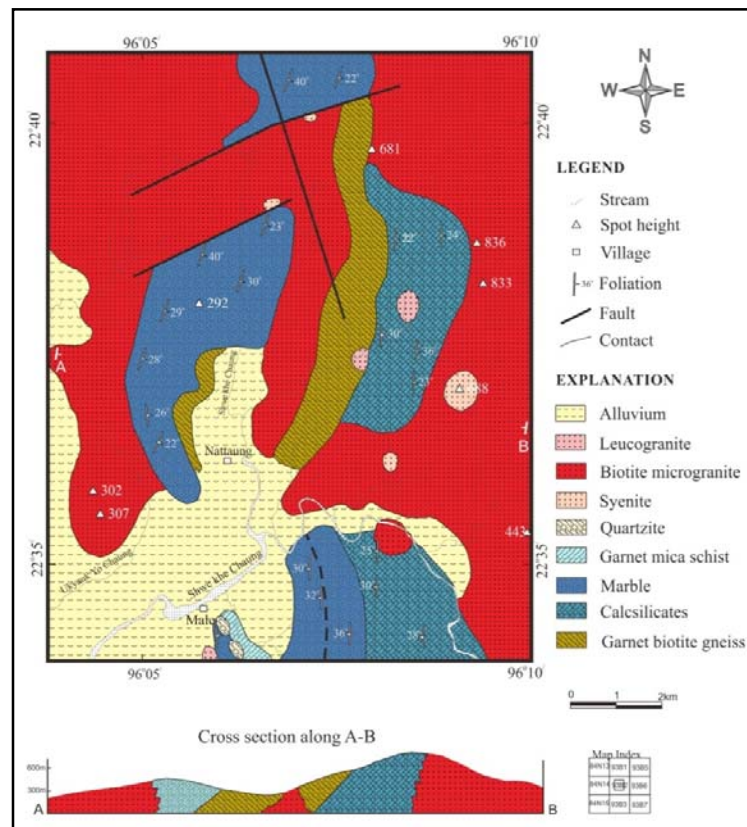


Figure (1). Geological Map of the Nattaung Area, Singu Township, Mandalay Region (after Maung Maung Naing, 1989; Khin Win Khaing, 2016).

Research Methods

More than thirty representative igneous rock samples were collected from the granitic rocks from the study area. The collected samples were then carefully selected for petrological and geochemical analyses. Nine igneous rock samples (6 granites and 3 leucogranites) have been selected for geochemical analysis. Major, minor and trace elemental composition were analyzed by X-Ray Fluorescence (XRF) Spectrometry. The XRF analyses were carried out at the Laboratory of Geology, University Research Center, University of Mandalay. The chemical analysis was made only for samples from fresh rocks which experienced neither

weathering nor metamorphism. Major and trace elemental data of the studied samples obtained by XRF analyses are described in Table (1). XRF whole-rock analysis data were used in classifying the rock type, in determining the magmatic affinity, and in discriminating of tectonic setting. The Standard CIPW norms for the analyzed rocks were calculated in a way to work out the mineralogy and classification of the rocks. The resulting normative compositions of the analysed samples are also given in Table (1).

Table (1). Chemical composition and calculated (CIPW) normative composition of intrusive igneous rocks (granite and leucogranite) from Nattaung Area

ID Rock type	Nt-01 Gr	Nt-06 Leu-Gr	Nt-12 Gr	Nt-16 Gr	Nt-18 Gr	Nt-19 Leu-Gr	Nt-27 Gr	Nt-28 Gr	Nt-31 Leu-Gr
SiO ₂	65.00	68.30	67.20	70.80	64.40	68.40	63.10	62.30	67.30
TiO ₂	0.36	0.10	0.39	0.31	0.38		0.36	0.65	0.14
Al ₂ O ₃	18.80	18.40	17.10	14.90	18.50	16.30	20.70	20.20	18.30
Fe ₂ O ₃	2.80	1.12	2.98	2.31	3.86	0.71	3.18	4.58	1.21
MnO	0.08	0.05	0.10	0.05	0.15	0.13	0.09	0.09	0.05
MgO	0.27	0.11	0.37	0.26	0.35	0.13	0.29	0.28	0.24
CaO	1.99	1.10	2.34	1.84	2.33	0.92	2.75	2.33	1.53
Na ₂ O	4.22	3.14	2.65	2.42	3.89	5.33	4.53	3.55	4.75
K ₂ O	6.07	7.55	6.07	6.45	5.62	7.64	4.49	5.55	6.30
P ₂ O ₅	0.13	0.08	0.31	0.18	0.13	0.14	0.15	0.12	0.11
SO ₃	-	-	0.33	0.06	0.03	0.04	0.03	0.03	0.02
Total	99.78	99.98	99.89	99.62	99.70	99.89	99.73	99.79	100.01
Rb ₂ O	0.03	0.04	0.04	0.03	0.03	0.05	0.03	0.04	0.03
SrO	0.05	0.02	0.04	0.05	0.06	0.01	0.06	0.05	0.02
Y ₂ O ₃		0.00	0.00	0.00	0.00	0.00	0.00	-	0.00
ZrO ₂	0.04	0.00	0.02	0.05	0.03	-	0.06	0.06	-
ZnO	0.01	-	0.01	0.01	-	-	0.01	0.02	-
BaO	0.12	-	0.01	0.01	0.01	-	0.01	0.02	-
Normative minerals									
Q	13.14	17.56	22.65	26.76	15.69	7.81	13.91	16.33	11.5
Or	35.52	44.55	36.47	38.87	32.84	44.45	26.12	32.43	36.77
Ab	36.92	27.93	23.79	21.84	34.06	43.16	39.56	30.72	41.6
An	9.02	4.98	9.85	8.25	10.75	-	12.62	10.78	6.84
C	2.07	3.57	2.98	1.14	2.28	-	4.05	4.84	1.33
Di	-	-	-	-	-	1.05	-	-	-
Hy	0.73	0.3	1.04	0.73	0.96		0.79	0.76	0.65
Wo	-	-	-	-	-	0.92	-	-	-
Ac	-	-	-	-	-	1.95	-	-	-
Il	0.12	0.08	-0.07	0.02	0.21	-	0.12	0.12	0.06
Hem	1.92	0.78	2.11	1.64	2.66	-	2.18	3.15	0.83
Ap	0.27	0.17	0.66	0.38	0.27	0.29	0.31	0.25	0.23
Hl	0.08	0.05	0.08	0.06	0.09	0.22	0.09	0.16	-
Zr	0.04	-	0.02	0.05	0.03	-	0.05	0.05	-
Pr	-	-	0.12	0.02	0.01	0.01	0.01	0.01	0.01
Ru	0.19	0.03	0.31	0.21	0.16	-	0.19	0.39	0.06
AN	19.63	15.14	29.29	27.41	23.99	0	24.19	25.98	14.13
DI	13.58	16.06	13.61	14.91	13.1	16.26	11.64	12.81	14.48
Mg#	0.276	0.28	0.33	0.308	0.264	0.42	0.265	0.195	0.44

Note: Gr-granite; Leu-Gr-Leucogranite; Mg# -Magnesium number, “-” denote below detection limit

Results and Discussion

Although the research area is comprised of granite and its associated rocks such as biotite microgranite, syenite, leucogranite, aplite and pegmatite, this study only focuses on biotite microgranite and leucogranite which are the major igneous rock units exposed in the area based on petrographic examination and geochemical analysis.

Petrography of granitic rocks

Biotite Microgranite

Megascope study: Biotite microgranite is hard and compact. The rocks show dark grey to light grey on weathered surface, however it exhibits milky white or whitish on fresh surface. It has medium grained texture and mainly composed of quartz plagioclase and biotite. Biotite generally occurs as dark brown small flakes.

Microscopic study: Microscopically, biotite-microgranite mostly contains quartz, orthoclase, plagioclase, biotite, muscovite and other accessory minerals (Fig.2a and b). Quartz commonly occurs as anhedral interstitial grains. Orthoclase occurs as subhedral grains and displays as simple twin. The untwinned orthoclase is common. Lesser amount of twinned plagioclase also present in thin section. Plagioclase (albite) shows inclined extinction and zoning sometimes present in some albite crystals. This medium-grained equal-granular rock shows hypidiomorphic granular texture. Although quartz occurs as primarily constituents, it is sometimes formed as inclusions within the plagioclase feldspar. Orthoclase and microcline are observed as medium grained crystals characterized by subhedral forms.

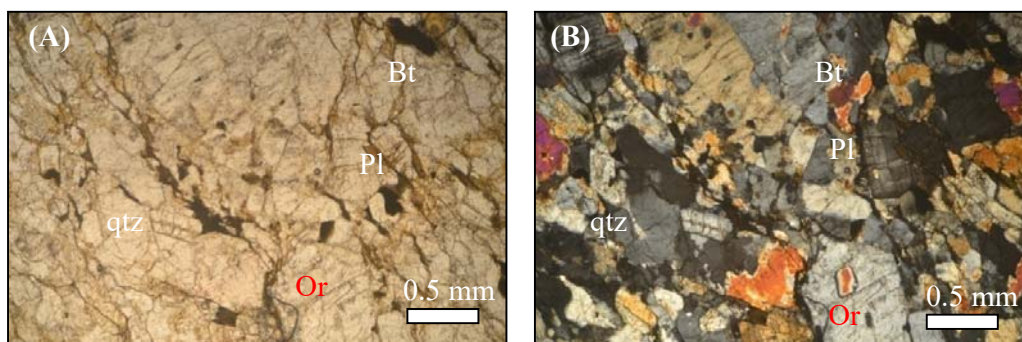


Figure (2). Photomicrograph of biotite microgranite (a) under PPL and (b) under XN. Q- quartz, Pl-plagioclase, Or-orthoclase, Bt-biotite.

Leucogranite

Megascope study: Leucogranite mainly consists of quartz and feldspar (Fig.3a and b). It is very coarse-grained, hard and compact. The rock shows reddish color on weathered surface whilst it displays milky white to white color on fresh surface.

Microscopic study: Leucogranite is mainly composed of quartz, orthoclase feldspar, albite with minor amount of muscovite. It is fine- to medium-grained and exhibits hypidiomorphic granular texture. Quartz occurs as anhedral to subhedral grains. Fairly large perthite grains are occasionally found in association with andulose quartz. It usually occurs as interstitial crystals and sometimes occurs as an intergrowth with quartz.

The modal compositions of intrusive igneous rocks are estimated based on petrographic examination (Table 2) and plotted on the QAPF diagram of Streckeisen (1976) (Fig.4). This diagram is intended for general classification of granitic rocks from Nattaung

area. This diagram indicates that the granitic rocks from Nattaung area are plotted in granite field of QAPF diagram except one sample which falls within the alkali feldspar granite field (Fig.2).

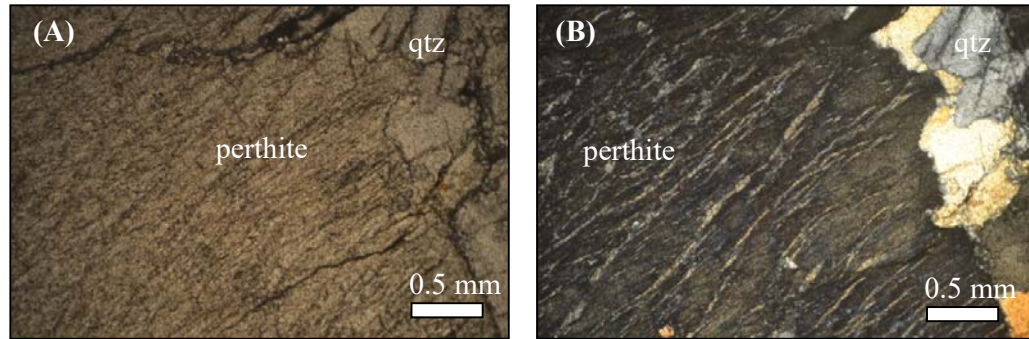


Figure (3). Large crystal of perthite and undulose quartz in the leucogranite (a) Under PPL and (b) under XN. Qtz-Quartz.

Table (2). Estimated modal composition of biotite microgranite and leucogranite from petrographic microscopy.

No.	Samples ID	Rock type	Qtz	Kfls	Pl	Bt	Ms	Hb	others	total
1	Nt-01	Biotite microgranite	29	45	11	12	-	1	2	100
2	Nt-12	Biotite microgranite	32	44	12	8	-	2	2	100
3	Nt-16	Biotite microgranite	35	48	10	6	-	-	1	100
4	Nt-18	Biotite microgranite	30	42	13	12	-	1	2	100
5	Nt-27	Biotite microgranite	31	40	15	13	-	-	1	100
6	Nt-28	Biotite microgranite	34	43	12	11	-	-	-	100
7	Nt-06	Leucogranite	32	55	7	-	5	-	1	100
8	Nt-19	Leucogranite	40	53	1	-	6	-	-	100
9	Nt-31	Leucogranite	42	45	9	-	3	-	1	100

Note: Qtz-quartz, Kfls-K-feldspar, Pl-plagioclase feldspar, Bt-biotite, Ms-Muscovite, Hb-hornblende

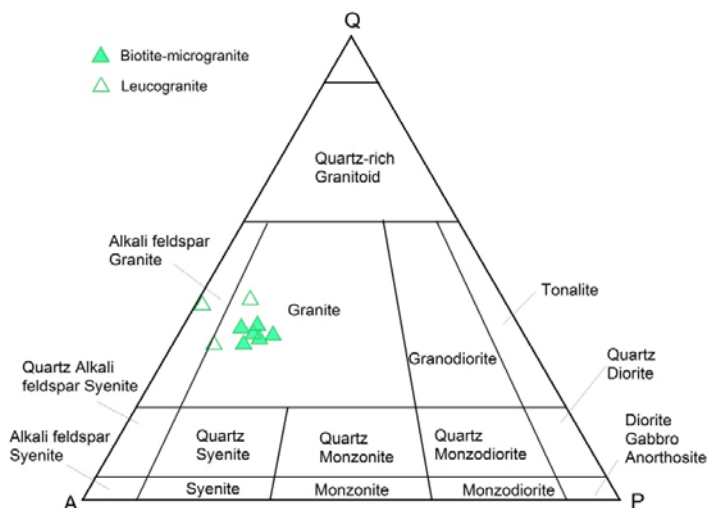


Figure (4). QAPF modal classification diagram of granitic rocks from Nattaung area (after Streckeisen, 1976). Representative samples from tables 2 are plotted. Sample names are omitted for clarity.

Geochemical Characteristics of the Granitic Rocks

Chemical classification of granitic rocks is based on major and minor oxides data obtained from the XRF analysis.

SiO₂ content in the studied granitic rocks ranges from 65 to 70.8 %. Based on the silica percentage data, the magma responsible for the formation of granitic rocks of the study area is acidic in composition. The total alkali versus silica (TAS) diagram divides the igneous rocks into ultrabasic, basic, intermediate and acid, on the basis of silica content. Plot on the TAS diagram (Cox et al., 1979) indicates that the bulk compositions of intrusive rocks of Nattaung are fall within the fields of granite and syenite (Fig.5). Nattaung granitic rocks samples were also classified according to normative An-Ab-Or composition (Barker, 1979). On the An-Or-Ab diagram, all the rock samples fall within the granite field (Fig. 6).

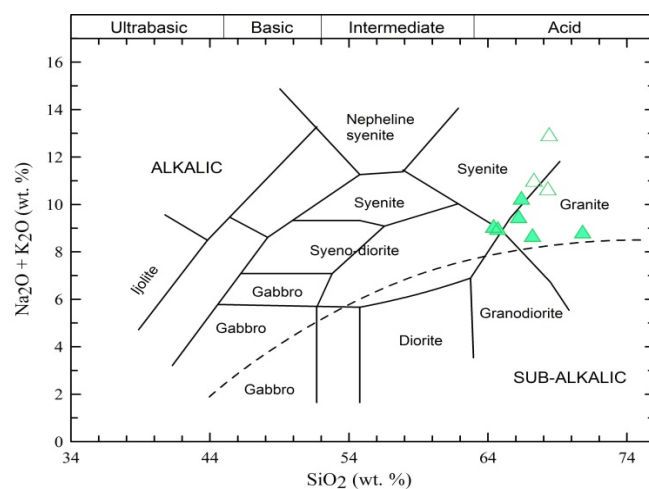


Figure (5). Chemical classification of granitic rocks using total alkali versus silica (TAS) diagram (Cox et al., 1979). Representative samples from tables 1 are plotted. Sample names are omitted for clarity. Symbols as in figure 4.

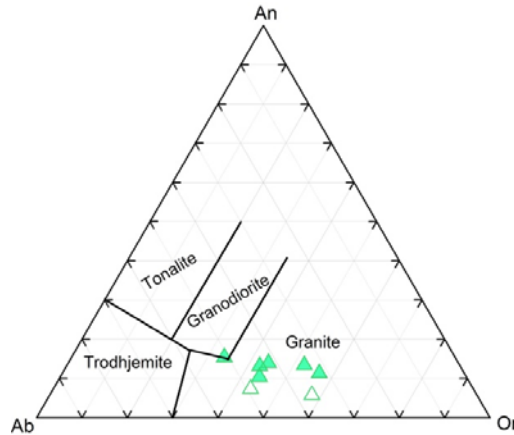


Figure (6). Normative albite-orthoclase-anorthite digram for the granitic rocks of the study area (Barker, 1979). Representative samples from Table 1 are plotted. Sample names are omitted for clarity. Symbols as in figure 4.

Igneous rocks can be sub-divided into two major magma series: the alkaline and sub-alkaline series. The granitic rock samples of Nattaung area were plotted on the R1-R2 classification diagram of De la Roche et al. (1980) and, on the diagram they fall within the sub-alkaline magma series (Fig. 7)

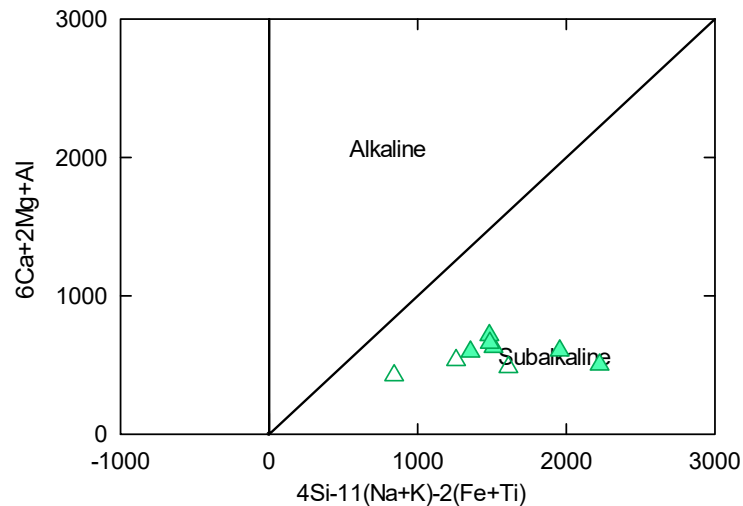


Figure (7). The subdivision of plutonic into alkaline and sub-alkaline magma series using the parameters R1 and R2 (after De la Roche et al., 1980), calculated from millication proportions. $R1=4Si-11(Na+K)-2(Fe+Ti)$; $R2= 6Ca+2Mg+Al$. Representative samples from Table 1 are plotted. Sample names are omitted for clarity. Symbols as in figure 4.

The sub-alkaline igneous rocks are divided into the calc-alkali and tholeiitic series on the basis of their iron contents in the AFM plot (Irvine and Baragar, 1971), where $A=Na_2O+K_2O$, $F=FeO+0.8998 \times Fe_2O_3$, and $M=MgO$. For the extreme felsic igneous rocks, typically granitic rocks, there is no satisfactory way of distinguishing calc-alkaline and tholeiitic member (Philpotts, 2009). However, the granitic rocks from Nattaung area are plotted on the AFM diagram (Fig. 8a) and they fall within the calc-alkaline field. Bi-variate

plot of An content of normative plagioclase versus Al_2O_3 (wt. %) also indicate that the granitic rocks falls within the calc-alkaline magma series (Fig. 8b).

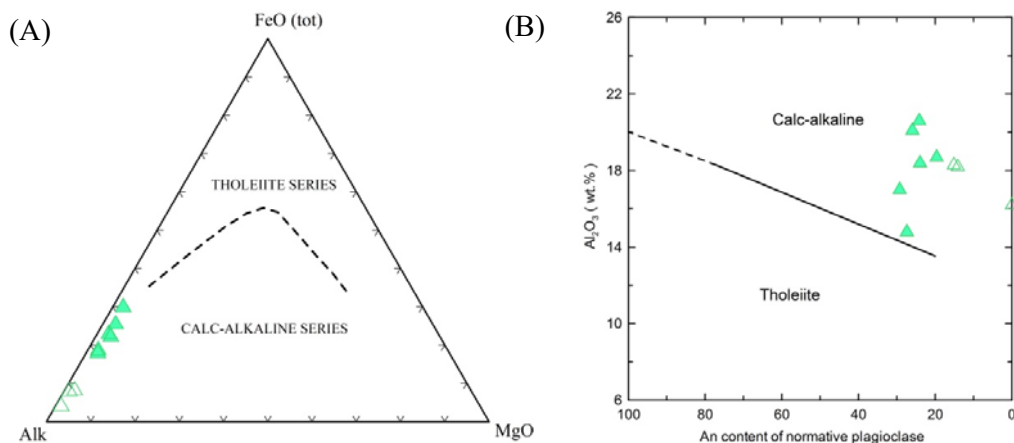


Figure (8). (a) AFM plot of the intrusive and basaltic rocks from the Nattaung area. The separating line for the field of tholeiitic and calc-alkaline rocks is from Irvine and Baragar (1971). $A = \text{Na}_2\text{O} + \text{K}_2\text{O}$, $F = \text{FeO} + 0.8998 \times \text{Fe}_2\text{O}_3$, and $M = \text{MgO}$. (b) The subdivision of tholeiitic and calc-alkaline rocks by using An content of normative plagioclase versus Al_2O_3 . Representative samples from Table 1 are plotted. Sample names are omitted for clarity. Symbols as in figure 4.

Alumina saturation of the rocks was also defined by using the Al_2O_3 -CaO-($\text{Na}_2\text{O} + \text{K}_2\text{O}$) diagram (Fig. 9a) (Hyndman, 1985). The granitic rocks fall within the peraluminous field.

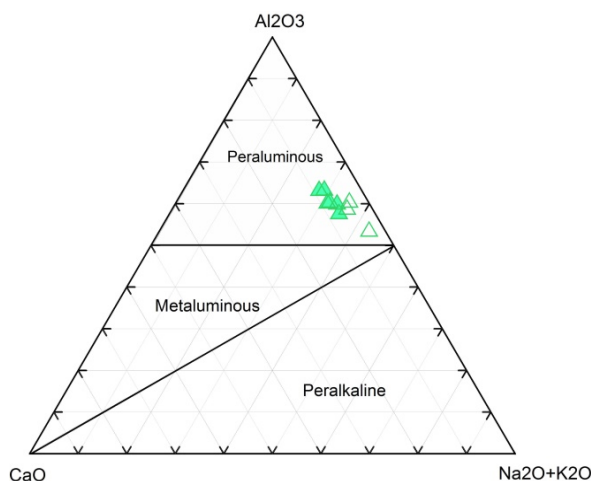


Figure (9). ACF diagram for the granitic rocks of the study area (after Hyndman, 1985). $A = \text{Al}_2\text{O}_3 + \text{Na}_2\text{O} + \text{K}_2\text{O}$, $C = \text{CaO}$, $F = \text{Fe}_2\text{O}_3 + \text{MgO}$. Representative samples from Table 1 are plotted. Sample names are omitted for clarity. Symbols as in figure 4.

For the types of granitoids or granite, various plots are used to distinguish I- and S-type. ACF diagram (Figure 10a) indicates that igneous rocks from the study area belong to S-type. On the plot of Shand's diagram (Shand, 1927), the majority of granitic rock samples fall in the S-type field (Figure 10b).

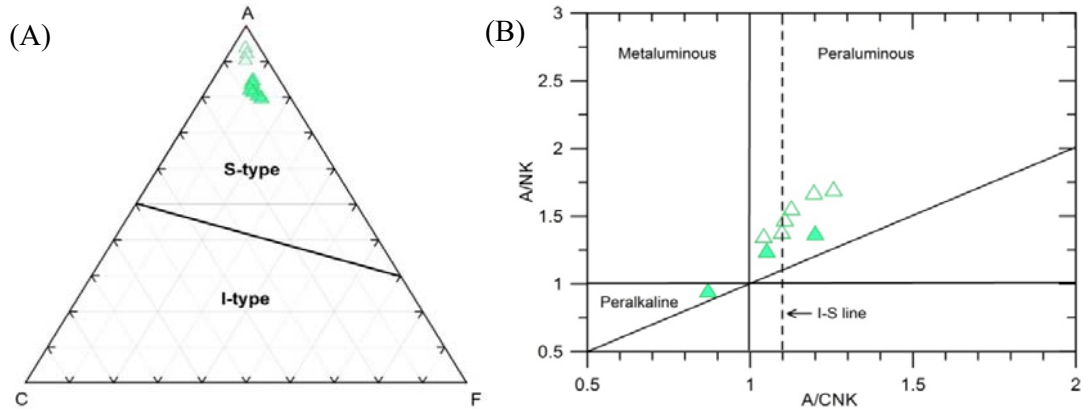


Figure (10). (a) ACF diagram for the granitic rocks of the study area. Molar ratios: A- $\text{Al}_2\text{O}_3 + \text{Na}_2\text{O} + \text{K}_2\text{O}$; C-CaO; F- $\text{Fe}_2\text{O}_3 + \text{MgO}$ (after Hydman, 1985) (b) Alumina/alkali index diagram (Shand, 1927) for the granitic rocks from the study area. A/CNK = molar ratio $\text{Al}_2\text{O}_3 / (\text{CaO} + \text{Na}_2\text{O} + \text{K}_2\text{O})$, A/NK = (molar ratio $\text{Al}_2\text{O}_3 / \text{Na}_2\text{O} + \text{K}_2\text{O}$) Representative samples from Table 1 are plotted. Sample names are omitted for clarity. Symbols as in figure 4.

Variation Diagrams

Variation diagrams were constructed for the studied granitic rocks by plotting the major and minor oxide data against SiO_2 in order to see variation among them (Fig.10). On the Harker' diagram (Fig.11), SiO_2 is positively correlated with K_2O whereas other major and minor oxides such as CaO, FeO, Al_2O_3 and TiO_2 are negatively correlated with the SiO_2 . Other oxides show no apparent correlation with the SiO_2 .

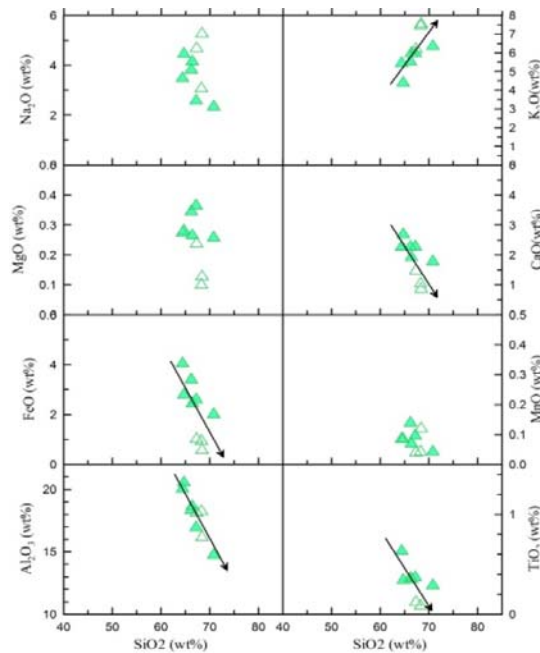


Figure (11). Harker variation diagram of intrusive igneous rocks from the Nattaung area. Arrows in the diagram indicate the correlation trend. Representative samples from Table 1 are plotted. Sample names are omitted for clarity. Symbols as in figure 4.

Petrogenesis

Tectonic Discrimination

Discrimination of the tectonic environment for the granites of the study area was based on the work of Maniar and Piccoli (1989). They classified the granitic rocks into two main groups: Orogenic and An-orogenic. The former contains Island Arc Granitoid (IAG), Continental Arc Granitoid (CAG), Continental Collision Granitoid (CCG) and Post Orogenic Granitoid (POG). The latter consists of Rift-Related Granitoids (RRG), Continental Epirogenic Uplift Granitoids (CEUG) and Oceanic Plagio-granite (OP). Tectonic environments for the granitic rocks are usually discriminated by means of major and minor element chemistry. In this scenario, various discrimination diagrams were applied for igneous rocks of the Nattaung area and sequentially discriminate various tectonic environments

K_2O versus SiO_2 diagram discriminates the IAG+CAG+CCG+ RRG+CEUG and OP field. In this figure all of the igneous rocks from the study area fall within the IAG+CAG+CCG+ RRG+ CEUG field (Fig.12a). Al_2O_3 versus SiO_2 diagram (Fig.12b) attempts to plot the granitic rocks of the study area into IAG+CAG+CCG, RRG+CEUG and POG fields. According to this diagram all of the igneous rocks plot in IAG+CAG+CCG field. Moreover, on the MgO versus SiO_2 variation diagram (Fig.12c), all of the igneous rocks fall in the IAG+CAG+CCG field too. In the diagram of Maniar and Piccoli (1989) (Fig.13), however, most of the granites are confined to CAG and CCG fields.

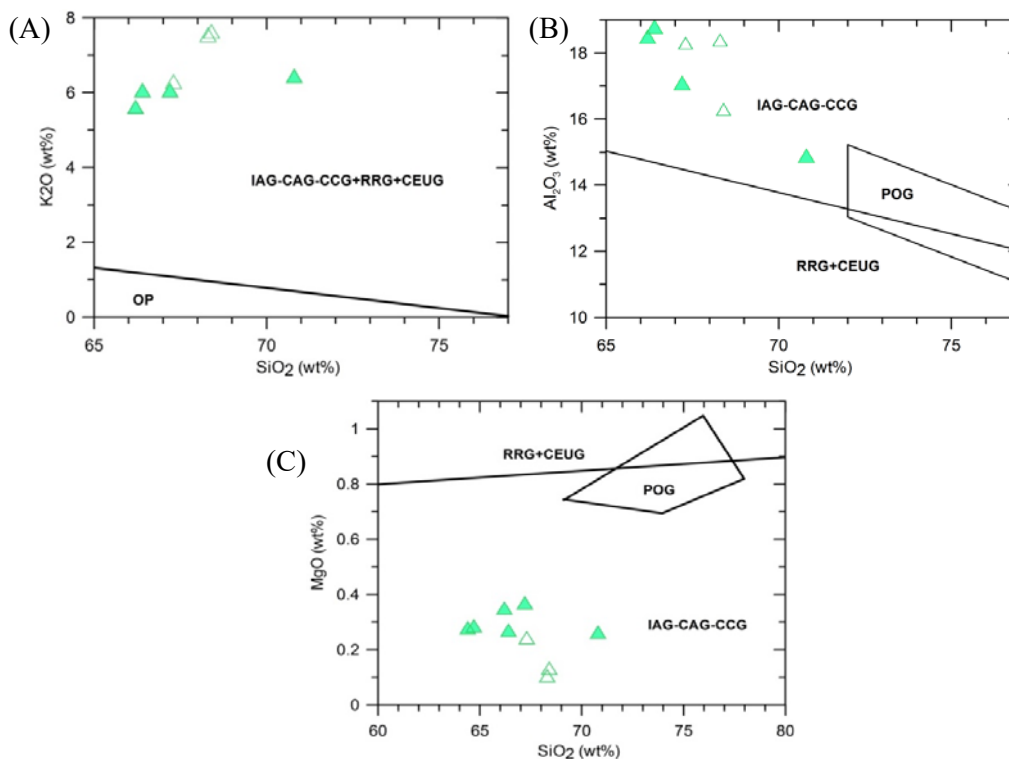


Figure (12). Tectonic discrimination diagrams for granitic rocks of Nattaung area (a) K_2O vs SiO_2 diagram (b) Al_2O_3 vs SiO_2 diagram and (c) MgO vs SiO_2 diagram (after Maniar & Piccoli, 1989). IAG-Island Arc Granitoid, CAG-Continental Arc Granitoid, CCG-Continental Collision Granitoid, POG-Post Orogenic Granitoid, RRG-Rift-Related Granitoids, CEUG-Continental Epirogenic Uplift Granitoids, OP-Oceanic Plagio-granite. Representative samples from Table 1 are plotted. Sample names are omitted for clarity. Symbols as in figure 4.

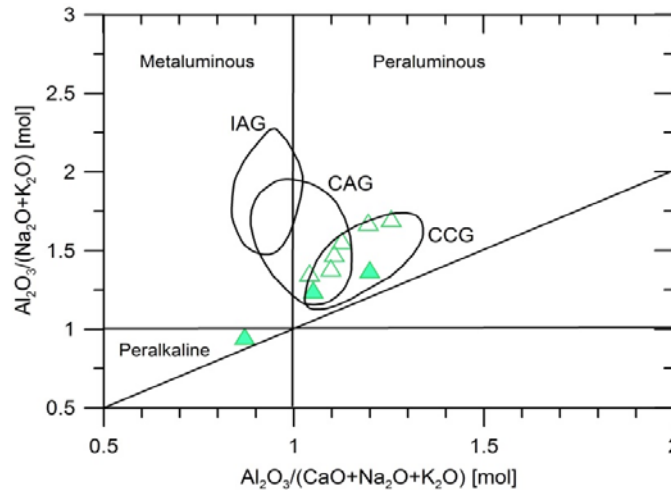


Figure (13). Diagram of Maniar and Piccoli (1989) applied to granitic rocks of Nattaung area. Granitic rock samples plot in continental arc granitoid (CAG) and Continental collision granitoid (CCG) fields. Representative samples from Table 1 are plotted. Sample names are omitted for clarity. Symbols as in figure 4.

According to the above criterion, it can be concluded that the granitic rocks from the Nattaung area fall in the IAG+CAG+CCG field which discriminate the granitic rocks of the study area as the orogenic granitoids.

Conclusions

The granitic rocks of the study area may be regarded as continental arc granitoids as well as continental collision granitoid. Hence, it seems reasonable that the granitic rocks were formed in the continent in relation to the subduction of an oceanic plate beneath the continent.

Mineralogical characteristics, and some chemical properties, for example, as already shown in ACF diagram, suggest that the granitic rocks from the study area are of mostly S-type. This was also supported by the occurrence of aluminium rich characters as well as from the mineralogy of the granite composition. Normative corundum of the granite is also greater than 1%. Therefore, it can be concluded that biotite microgranite and leucogranite were formed in the continent due to the subduction of an oceanic plate beneath the continent.

Field criteria suggest that biotite microgranite and leucogranite intruded within the highly-deformed metamorphic terrain of the study area. The emplacements of the igneous bodies took place by forceful intrusion. Minor Pegmatite and aplitic dykes were intruded within the biotite microgranite pluton as the later phases. Since the field relationships of the igneous and metamorphic rocks imply that the latest metamorphism immediately preceded the emplacement of the microgranite.

The depth of emplacement of igneous intrusions for the study area was deduced from the field evidences and petrochemical criteria. Temperature of the country rock (metamorphic rocks) of igneous intrusion is estimated to be greater than 450°C as they belong to the amphibolite to granulite facies. Granitic intrusions display mostly discordant structural relationship to the country rocks and no gradational contact between them was observed. Abundance of pegmatite bodies and aplite veins containing tourmaline, beryl, rubellite, garnet are observed in association with granitic rocks. Contact metamorphic zones were

rather localized and the chilled border zones are absent. Xenoliths of the country rocks are rather rare as well. Therefore, these criteria collectively suggest the mesozonal to epizonal characters of the granitic intrusion for the study area.

Acknowledgement

We want to express our acknowledgement to Dr Htay Win, Professor and Head of the Geology Department, Yadanabon University, for his kind permission to prepare this manuscript. Sincere thanks are given to the Rector Dr Maung Maung Naing and Pro-Rectors, Dr Si Si Khin and Dr Tint Moe Thu Zar, Yadanabon University, for giving us the opportunity to submit this manuscript to MNCES 2019.

References

- Barker, F. (1979) Trondhjemite: definition, environment and hypotheses of origin, in: Barker, F. (ed.), *Trondhjemites, Dacites and Related Rocks*, Elsevier Amsterdam, 1-12.
- Barley, M. E., Pickard, A. L. Khin Zaw, Rak, P. & Doyle, M. G. 2003. Jurassic to Miocene magmatism and metamorphism in the Mogok metamorphic belt and the India-Eurasia collision in Myanmar. *Tectonics*, 22, doi: 10.1029/2002TC001398.
- Bertrand, G., Rangin, C., Maluski, H., Han, T.A., Thien, M., Myint, O., Maw, W., Lwin, S., 1999. Cenozoic metamorphism along the Shan scarp (Myanmar): evidence for ductile shear along the Sagaing fault or northward migration of the eastern Himalayan syntaxis? *Geophysical Research Letters* 26, 915–918.
- Bertrand, G., Rangin, C., Maluski, H., Bellon, H., Scientific Party, G.I.A.C., 2001. Diachronous cooling along the Mogok metamorphic belt (Shan scarp, Myanmar): the trace of the northward migration of the Indian syntaxis. *Journal of Asian Earth Sciences* 19, 649–659.
- Cox, K.G.J.D., Bell and Pankhurst, R.J. 1979. *The interpretation of igneous rock*, George Allen and Unwin, London. 464p.
- De la Roche, H., Leterrier, J., Grande Claude, P. & Marchel, M. 1980. A classification of volcanic and plutonic rocks using R1–R2 diagrams and major element analyses – its relationship and current nomenclature. *Chemical Geology* 29, 183–210.
- Hyndman, D.W. 1985. *Petrology of igneous and Metamorphic Rocks*, New York. Mc Graw- Hill, Inc; 2nd ed: 786p.
- Irvines, T.N. Baragar, W.R.A., 1971. A guide is the geochemical classification of the common volcanic rocks. *Can. J. Earth Sci.* 8, 523-548.
- Khin Win Khaing, 2015, Geochemistry and Petrology of the Igneous Rocks in Nattaung Area, Singu Township, Mandalay Region, MSc (Thesis) (unpublished), Geology Department, University of Mandalay.
- Maniar, P. D. & Piccoli, P. M. 1989. Tectonic discrimination of granitoids. *Geological Society of America Bulletin* 101, 635–643.
- Mitchell, A. H. G. 1993. Cretaceous-Cenozoic Tectonic Events in the Western Myanmar (Burma)-Assam Region. *Jour. Geol. Soc. Condon.* 150, 1090-1102.
- Mitchell, A. H. G., Myint Thein Htay, Kyaw Min Htu, Myint Naing Win, Thura Oo, Tin Hlaing., 2007. Rock relationships in the Mogok metamorphic belt, Tatkon to Mandalay, central Myanmar. *Journal of Asian Earth Science* 29, 891-910.
- Maung Maung Naing 1989. Geology of the Letpanhla-Nattaung Area, (Unpublished M.Sc Thesis, University of Mandalay).
- Philpotts, A. R. & Ague, J. J. 2009. Principles of igneous and Metamorphic Petrology, 2nd edition, Cambridge University Press. pp.684.
- Searle, D.L and Ba Than Haq, 1964. The Mogok Belt of Burma and its relationship to the Himalayan Orogeny, Proc 22nd. Inter. Geol. Congr. P 11. P 20.
- Streckeisen, A. L. 1976, To each plutonic rock its proper name. *Earth Sci. Rev.*, 12,1 -33.
- Shand, S.J., 1927. *Eruptive Rocks*. D. Van Nostrand Company, New York, pp. 360.